

This Page Is Inserted by IFW Operations
and is not a part of the Official Record

BEST AVAILABLE IMAGES

Defective images within this document are accurate representations of the original documents submitted by the applicant.

Defects in the images may include (but are not limited to):

- BLACK BORDERS
- TEXT CUT OFF AT TOP, BOTTOM OR SIDES
- FADED TEXT
- ILLEGIBLE TEXT
- SKEWED/SLANTED IMAGES
- COLORED PHOTOS
- BLACK OR VERY BLACK AND WHITE DARK PHOTOS
- GRAY SCALE DOCUMENTS

IMAGES ARE BEST AVAILABLE COPY.

**As rescanning documents *will not* correct images,
please do not report the images to the
Image Problem Mailbox.**



DECLARATION

I, Toshihiro Ando, a national of Japan, c/o National Institute for Materials Science, 2-1, Sengen 1-chome, Tsukuba-shi, Ibaraki 305-0047 Japan, one of the inventors of USSN. 09/926,188 do hereby solemnly and sincerely declare:

(1) THAT the attached is the REFERENCE FIGURES AND ITS EXPLANATION to prove the substrate surface can be obtained in which steps of each mono atomic layer are arranged in series by, in accordance with the present invention, polishing a diamond (100) substrate in the range of 1.5 to 6 degrees, and hydrogen plasma treating said substrate. And

(2) THAT this attached document is for the purpose of the explanation that the diamond thin film growth takes place by step-flow growth mechanism by using this substrate, and therefore the S doped n type diamond of the present invention has the crystal perfect-ness which can not be realized by prior art. And

(3) THAT the above-mentioned REFERENCE FIGURES are the graphics made from the data measured by AFM(inter-atomic force microscope) treating on Sep 10, 2003 by myself by the described conditions in order to prove that the substrate of the present invention possesses the crystal perfect-ness which can not be realized by prior art.

And, I, Toshihiro Ando, being sworn state that the facts set forth above are true.

Signed this 13th April, 2004

Toshihiro Ando
Toshihiro Ando

Received at: 4:54AM, 4/19/2004

FROM 平山特許事務所/HIRAYAMA & CO. 0333522150

2004年 4月19日(月)18:10/著稿18:04/文書番号5300903847 P 14

D 746

PHYSICAL REVIEW
B
CONDENSED MATTER

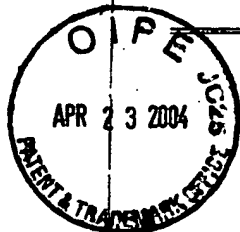
Published by
THE AMERICAN PHYSICAL SOCIETY
through the
American Institute of Physics

PHYSICAL REVIEW B

VOLUME 54, NUMBER 20

15 NOVEMBER 1996-II

ARTICLES



Molecular-orbital theory of monatomic and diatomic substitutional defects as shallow *n*-type dopants in diamond

Alfred B. Anderson and Emilia J. Grantscharova*

Chemistry Department, Case Western Reserve University, Cleveland, Ohio 44106-7078

John C. Angus

Department of Chemical Engineering, Case Western Reserve University, Cleveland, Ohio 44106-7217

(Received 13 May 1996)

A survey of potential shallow *n*-type donors in diamond was performed using the atom superposition and electron delocalization molecular-orbital method. Electronic structure and defect stabilities were estimated for N, P, O, S, F, and Cl in substitutional monovacancy sites; I, Xe, and the atom pairs BO, BS, NO, NS, and BeCl were studied on substitutional divacancy sites. The calculations indicate that the BS, NS, and BeCl pairs and I in divacancy sites may provide shallow donor levels, and may be more stable than P in a monovacancy site. [S0163-1829(96)0144-2]

I. INTRODUCTION

The experimental search for shallow *n*-type diamond continues. It is well understood that a main group atom with five valence electrons will, when substituting for a carbon atom in the diamond lattice, be a donor.^{1,2} Substitutional nitrogen is known from measurement to be a deep optical donor (absorption edge at 2 eV) and a deep thermal donor (activation energy 1.6–1.7 eV).³ Theoretical calculations concur,^{4,5} and show how one C-N bond increases in length from the diamond value of 1.54 Å to about 1.99 Å, while the other three bonds are compressed to about 1.48 Å, in a trigonal distortion. Phosphorous, the neighbor of nitrogen in the period below, is predicted to be a shallow donor.^{4,5} This is due to the large size of the 3p valence orbitals that overlap the 2p orbitals of the neighboring carbon atoms strongly, even in the relaxed structure. The P-C antibonding σ* orbital that is occupied with the extra electron can, at most, drop only a little beneath the bottom of the conduction band, and the trigonal distortion is small (in Ref. 5 three P-C bond distances are calculated to be increased by 0.06 Å, and the fourth by 0.09 Å). This makes phosphorous potentially interesting as a substitutional *n*-type dopant in diamond, but it will be difficult to incorporate it because it is relatively unstable. In Ref. 3 it was calculated to bind in a diamond monovacancy site about 10 eV more weakly than a carbon atom, whereas a nitrogen atom was calculated to bind only 4 eV more weakly than the carbon atom. The weakness of the P-C bonds is caused by the promotion of the phosphorous 3p electron from its level, which is close to the bottom of the diamond band-gap region, to the top of the gap region. An additional factor is the energy of compression of surrounding P-C and C-C bonds from their single bond equilibrium values. Because of the expected relative instability of phosphorous in diamond, it is not surprising that attempts to incorporate it by introducing compounds into the low-pressure

growth medium have not yielded encouraging results.^{4–8} Recently, however, it has been reported that mild cold implantation of phosphorous ions followed by rapid annealing yielded *n*-type diamond with a low 0.2-eV activation energy for electron promotion to the conduction band.⁹ This gives some hope for phosphorous. Also interesting is the recent report that phosphorous will codope with nitrogen during low-pressure diamond growth.¹⁰ Such systems have, however, not demonstrated *n*-type conduction or phosphorous-related luminescence. In these systems the nitrogen concentration is about equal to or greater than that of phosphorous. If both dopants exist as substitutional atoms, perhaps all substitutional P are oxidized to P⁺. An equal number of substitutional N would be reduced to N[−] with two band-gap electrons to give a longer C-N bond σ* orbital with an energy even deeper in the band gap. Alternatively, substitutional PN dimers, if they form, might be deep donors. A theoretical study using the methods of this paper has, in fact, supported this interpretation of the lack of electrical activity and luminescence.¹¹

Arsenic has also been implanted in diamond^{12,13} and Rutherford backscattering spectroscopy indicated that ~40–50 % of the As atoms were located in substitutional sites. Such structures should be highly stressed because of the large size of the As atom, and they will be donor defects. Measurements of the electrical behavior indicated the formation of a semiconducting surface layer with a 0.41-eV activation energy.¹⁴ However, similar results were obtained for the implantation of Ne and Na, indicating that lattice defects caused by the implantation may be responsible for the observed electrical properties.

Interstitial atoms, except for H, which has been predicted to act both as a deep donor and a deep acceptor,¹⁵ are expected to be shallow donors in diamond. The large overlap of the interstitial atom orbitals and the neighboring carbon atom orbitals result in substantial destabilization of the occupied

TABLE I. Atomic parameters used in the calculations. Principal quantum numbers n , Slater orbital exponents ζ (a.u.), and diagonal Hamiltonian matrix elements H (eV).

Atom	s			p		
	n	ζ	H	n	ζ	H
H	1	1.2	-13.6
Be	2	1.0060	-10.822	2	1.0060	-8.100
B	2	1.2881	-13.930	2	1.2107	-9.298
C	2	1.8174	-16.590	2	1.7717	-11.260
N	2	1.9237	-18.330	2	1.9170	-12.530
O	2	2.2458	-29.480	2	2.2266	-14.620
F	2	2.5638	-39.850	2	2.5500	-19.420
Al	3	1.3724	-10.620	3	1.3555	-5.986
P	3	1.8806	-17.650	3	1.6288	-11.990
S	3	2.1223	-22.200	3	1.8273	-12.360
Cl	3	2.3562	-26.540	3	2.0388	-15.010
I	5	2.9790	-24.610	5	2.6790	-14.450
Xe	5	3.1433	-23.700	5	2.8439	-13.440

σ^* orbitals, which will lie near or above the bottom edge of the conduction band, despite the repulsive forces that serve to push the neighboring carbon atoms off their lattice sites.^{4,5} Thus quantum calculations predict that interstitial Li (Refs. 4 and 5) and Na (Ref. 4) are shallow donors. By contrast, substitutional Li is predicted to be a shallow acceptor.⁵ Photoemission measurements with indiffused Li show the presence of acceptor levels 1.0–1.5 eV above the valence-band edge.⁶ These levels might be due to interstitial H,¹⁵ substitutional Li^{4,16} or something else, but currently there is no proven answer, and experimental investigations continue.²

II. RATIONALE FOR SYSTEMS STUDIED HERE

We examine the properties of selected atoms in monovacancy and divacancy substitutional sites and selected pairs of atoms in divacancy sites, with a view toward identifying shallow donors for diamond. Defect stabilities, electronic structures, and the effects of structural relaxation on optical and thermal excitation energies are calculated. For the monovacancy substitutional sites we consider N, P, O, S, F, and Cl. Oxygen and sulfur, from group VI B, have two electrons that will be promoted into the band gap, and F and Cl, from group VII B, have three. Whether these are deep or shallow donors should depend on the electron count and the orbital sizes,^{1,3} and this study addresses these issues. Although they were studied previously, N and P, from group V B, are included for comparison.

We also studied the incorporation of large single atoms and pairs of atoms into divacancy sites. A divacancy site has six dangling orbitals extending into the cavity, compared to four for a single-vacancy site, and there is one electron for each orbital. Such vacancies could act as traps for interstitial H, as we discussed in a previous paper.¹³ In the present context we are interested in characterizing the binding of atoms within these divacancy sites. We consider the resulting defect electronic structures in terms of orbital correlations of the dangling vacancy orbitals with the orbitals of atoms introduced into the vacancies, as in our earlier work involving

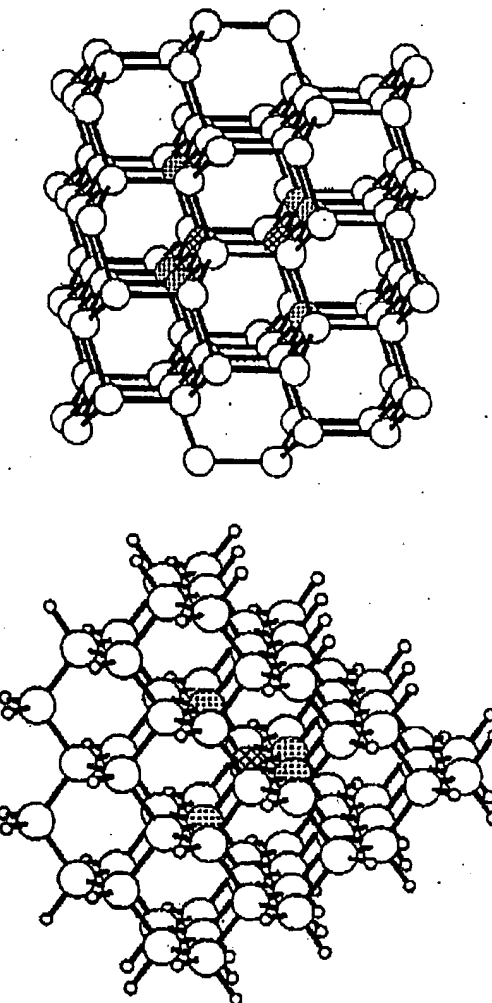


FIG. 1. Bulk superimposable C_{71} and C_{98} cluster models used for defect studies. The cross hatched central atoms are removed to create vacancy sites or replaced by foreign atoms to create substitutional defects. Nearest-neighbor (shaded) atoms around the defects are allowed to relax in the (111) directions. The dangling surface-orbital-terminating H atoms are not shown for the C_{98} cluster.

substitutional B and N.¹ Just as an atom with five valence electrons, such as N and P will, when in a monovacancy site, promote one electron into the band gap, an atom with seven valence electrons, such as I, will promote an electron into the band gap when in a divacancy site. Whether such an I atom is a shallow donor depends on the strengths of the orbital overlaps. We have explored this issue for I and also Xe, which will promote two electrons into the gap when in a divacancy site. Finally, for a diatom pair placed in a divacancy site, the electronic structure can be thought about in two ways. For example, BO is isoelectronic to CN, and so adding it to a divacancy site is similar to adding N to a

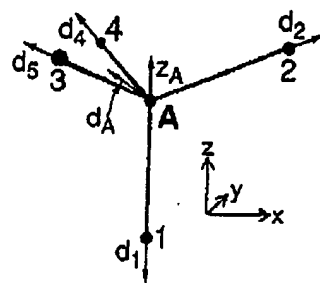


FIG. 2. Structure variables for the monovacancy and monosubstitutional atom sites.

monovacancy site. Alternatively, if we recognize that, when present in the diamond lattice, there will be a single σ bond between B and O, the remaining seven valence electrons will be in orbitals that will form bonding and antibonding counterparts with the six divacancy dangling orbitals containing six electrons, thus promoting an electron into the gap. In either viewpoint, one electron will be promoted into the band gap or above, and the specific properties of the atom will determine whether the defect is a shallow donor. In this regard we examine BO, BS, and BeCl as potential donors with one electron in a single orbital promoted into the band gap, and NO and NS with three electrons in two orbitals promoted into the gap.

III. THEORETICAL APPROACH

The atom superposition and electron delocalization molecular orbital (ASED-MO) theory¹⁷ was employed for this study. This is a semiempirical theory for calculating structures and electronic properties of molecules and solids from atomic data, namely, valence atomic orbitals and ionization potentials. The theory is based on partitioning the electronic charge density distribution function into atomic and delocalization (due to forming bonds) components ρ_a and ρ_d , respectively.

$$\rho = \sum_{\text{atoms}} \rho'_a + \rho_d. \quad (1)$$

TABLE II. Calculated binding energies, BE (eV), for atoms to vacancy sites and structure parameters as defined in Fig. 2 for the optimized trigonal and tetragonal defect structures. All displacements (z and d) and internuclear distances (R) are in Å units. Atoms that are next-nearest neighbor to substitutional atoms A are constrained to the bulk diamond lattice sites.

Atom	Trigonal						Tetragonal					
	BE	z_A	d_1	$d_{2,3,4}$	R_{A-1}	$R_{A-2,3,4}$	BE	d_A	$d_{1,2}$	$d_{3,4}$	$R_{A-1,2}$	$R_{A-3,4}$
N	10.7	0.235	0.224	-0.007	1.999	1.471	9.60	0.189	-0.006	0.135	1.791	1.434
O	7.05	0.347	0.216	-0.011	2.113	1.450	6.09	0.355	0.234	0.007	2.000	1.373
F	2.67	0.267	0.236	0.326	2.044	1.795	3.66	0.507	0.214	0.075	2.088	1.386
P	4.78	0.004	0.080	0.063	1.624	1.602	4.78	0.003	0.074	0.061	1.600	1.615
S	-5.67	0.184	0.475	0.186	2.199	1.674	-7.34	0.020	0.170	0.141	1.722	1.670
Cl	-10.03	0.420	0.223	0.144	2.183	1.623	-9.44	0.255	0.425	0.189	2.122	1.595

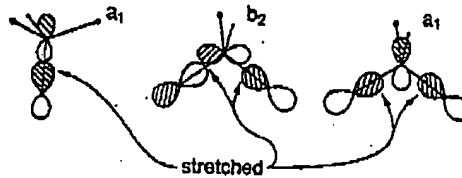


FIG. 3. Shapes of occupied σ^* orbitals for trigonally distorted N, O, and S substitutional defect centers (a_1 orbital on left), and for tetragonally distorted F and Cl substitutional defect centers (b_2 and a_1 orbitals on right).

Pairwise atom superposition energies E_{ab}^{ab} are calculated by integrating the electrostatic force on the nucleus of the less electronegative atom of each pair of atoms a and b , as they are brought into the molecular configuration. The sum E_R is called the atom superposition energy,

$$E_R = \sum_{a < b} E_{ab}^{ab}. \quad (2)$$

The electron delocalization energy E_D is the sum of integrals of the electrostatic force on the same nuclei as one atom after another is added to the cluster. This cannot be evaluated because the functional forms of ρ_d are generally not available, but E_D is sufficiently well approximated by a molecular-orbital electron delocalization energy ΔE_{MO} that the total energy

$$E = E_R + E_D \quad (3)$$

can be replaced by

$$E = E_R + \Delta E_{MO} \quad (4)$$

for many applications. The ΔE_{MO} that works in Eq. (4) is calculated using a modified extended Hückel Hamiltonian where diagonal matrix elements are set equal to the negative of measured atomic valence state ionization potentials, sometimes shifted for highly ionic systems. Off-diagonal elements for orbitals on the same atom are set to zero, and for orbital i on atom a and orbital j on atom b they are given as

$$H_{ij}^{ab} = 1.125(H_{ii}^{aa} + H_{jj}^{bb})\exp(-0.13R_{ab})S_{ij}^{ab} \quad (5)$$

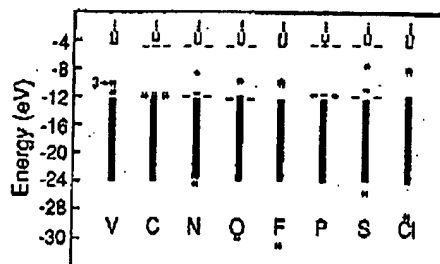


FIG. 4. Band-gap electronic structures calculated for the vacancy and for monosubstitutional atoms in the C_{70} clusters. The filled valence band is shaded and the empty conduction band is unshaded. Occupied band-gap orbital energy levels are shown for the vacancy V , which has four dangling orbitals with four electrons, and for the dopant atoms N through Cl. For N, O, F, S, and Cl, orbitals that are bonding between valence s and the cluster orbitals are shown beneath the valence band in energy.

where R_{ab} is the internuclear distance, S_{ij}^{ab} the overlap integral, and the H 's on the right-hand side are the diagonal matrix elements defined above.

The single- ζ Slater orbital exponent and diagonal matrix elements used in this work are in Table I. The carbon atom orbital exponents are those chosen to produce the C-C bond distance in graphite (1.42 Å) using the ASED-MO band program.¹⁸ The carbon atom diagonal H matrix elements are the negative of the measured $2s$ and $2p$ atom ionization potentials. With these parameters the calculated C-C bond distance from ASED-band calculations for diamond was 1.53 Å compared to the measured 1.54 Å. In the cluster models of this paper 1.54 Å is used for C-C distances except when there is relaxation included around the defects being studied. These carbon atom parameters yielded 8.05 eV per atom for the atomization energy of diamond in the ASED-band calculations, compared to an experimental determination of 7.35-eV per atom. The bulk modulus was calculated to be 539 GPa, which was within the range of experimental estimates, 442, 556, and 575 GPa. These results were similar

TABLE III. Calculated optical E_{optical} , relaxation E_{relax} , and thermal E_{thermal} activation energies (eV) for promoting an electron to the conduction band.

Defect	E_{optical}	E_{relax}	E_{thermal}
N	3.57	2.63	0.94
O	4.74	1.22	3.51
F	4.90	1.19	9.71
P	-0.21	1.14	-1.35
S	2.44	2.07	0.37
Cl	2.97	3.71	-0.79
SO	4.11	1.18	2.92
BS	-0.12	0.81	-0.93
NO	4.04	1.64	2.38
NS	3.09	3.12	-0.03
BeCl	2.41	2.31	0.11
I	0.95	1.09	-0.14
Xe	4.52	0.85	3.67

TABLE IV. Calculated structure parameters for $A^+(s)$. See Fig. 2 and caption to Table II.

Atom	z_A	d_1	$d_{2,3,4}$	R_{A-1}	$R_{A-2,3,4}$
N	0.000	-0.150	-0.015	1.525	1.525
O	0.277	0.242	-0.016	2.058	1.436
F	0.314	0.216	0.265	2.070	1.726
P	0.000	0.070	0.070	1.610	1.610
S	-0.005	0.147	0.155	1.683	1.697
Cl	0.229	0.419	0.141	2.188	1.619

to those calculated by density-functional band theory, 1.54 Å, 7.94 eV, and 438 GPa for the bond length, atomization energy, and bulk modulus, respectively.¹⁹ Generally, the single- ζ orbital exponents are chosen to fit molecular diatomic bond lengths. Thus the theory is parametrized for accuracy for bonded structures. The parameters for C, N, and P were used in Ref. 5, which can be consulted for further details.

IV. DIAMOND MODELS

We have used a $VC_{70}H_{60}$ cluster to model the single vacancy and an $AC_{70}H_{60}$ cluster to model a substitutional atom defect. For the divacancy and disubstitutional defect the $V_2C_{90}H_{78}$ and $ABC_{90}H_{78}$ clusters (Fig. 1) were used. Here V represents a single vacancy and A and B represent substitutional atoms. All defect structures were optimized by allowing neighboring C atoms to relax toward or away from the center of the vacancy site along $\langle 111 \rangle$ directions. For the clusters used, no surface atoms are relaxed for they are next-nearest neighbors to the defects. Comparison with previous calculations, wherein next-neighbor relaxations along $\langle 111 \rangle$ directions were allowed, showed 0.1–0.2 eV reductions in calculated binding energies of atoms to monovacancy sites, and in such cases cluster surface atoms were allowed to move.⁵ We feel the present model, which is computationally more efficient, is comparable to or better than the previous one. A few calculations of relaxations allowing deviations from the $\langle 111 \rangle$ directions of motions of relaxing atoms resulted in small ~ 0.1 -eV stabilizations that can be regarded as negligible at this level of modeling. Relaxation of atoms surrounding the monovacancy gives rise to a tetragonal dis-

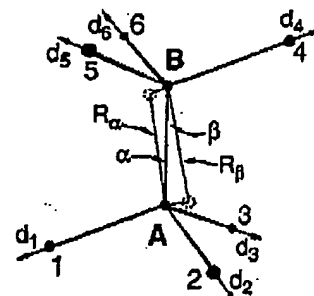


FIG. 5. Structure variables for divacancy and disubstitutional sites.

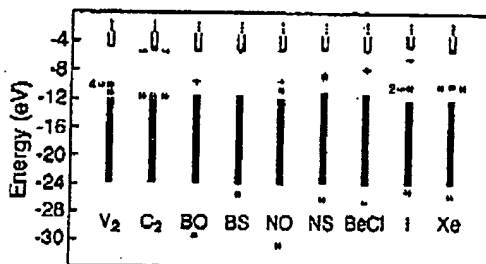


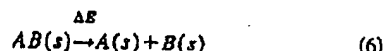
FIG. 6. Band-gap electronic structures for heteronuclear occupations of the adjacent divacancy site in the C_{96} cluster and also for I and Xe in this site. See caption to Fig. 4. The divacancy (V_2) has six dangling orbitals and six electrons.

tortion of C_{2v} symmetry with two C atoms relaxed away by 0.187 Å, the other two by 0.096 Å, and a stability gain of 0.36 eV. For the divacancy a stability of 0.89 eV comes with relaxation of the six surrounding C atoms to a structure with C_{2h} symmetry. This structure has an inversion center with, at each end, two C atoms relaxed away 0.094 Å, and the third by 0.171 Å. When the defect atoms are placed in the divacancy, the surrounding C atoms can experience large shifts in position; these shifts are related to the atom size and number of valence electrons as discussed below.

Energies for promoting band-gap electrons into the conduction band were determined in two ways. The optical energy was taken as the difference between the highest occupied band-gap orbital energy and the lowest empty conduction-band-orbital energy. The thermal energy was determined as the difference between the total energy of the defect cluster, with the structures relaxed as described above, and the total energy of the relaxed positively charged cluster plus the binding energy of an electron in the C-C bond stretched state as discussed in Ref. 5. There it is shown that the calculations favor localization of the promoted electron in this cluster and delocalization into the conduction band in the bulk. For cases of substitutional dimers the C_{98} cluster is used for this, and for monomers the C_{71} cluster is used with a stretched bond involving displacement of the central atom and a neighbor so that the defect has the same local structures as determined in Ref. 5 for the C_{96} cluster. To three figures after the decimal point the calculated electron affinities of these two clusters are the same.

We also determined the bonding energy of A and B in the divacancy site and isolated A and B in monovacancy sites

and the reaction energy for dissociation



where s stands for substitutional. The energy change for Eq. (6) was calculated using the total energies E of $C_{71}H_{60}$, $AC_{70}H_{60}$, $BC_{70}H_{60}$, $C_{98}H_{78}$, and $ABC_{96}H_{78}$:

$$\Delta E = E(C_{98}) + E(A(s)) + E(B(s)) - 2E(C_{71}) - E(AB(s)). \quad (7)$$

V. RESULTS AND DISCUSSION

A. Substitutional atoms: N, P, O, S, F, Cl

Though N and P were analyzed in the earlier paper,⁵ the calculations were repeated using the slightly different constraints of the present work for comparison and to establish trends. Structure parameters defining the substitutional atom defect structures are shown in Fig. 2. The central (substitutional) atom A has been allowed to move up (+z) and down (-z) with respect to the lattice point at z=0, giving rise to trigonal distortions and along the line in the xz plane (d_A) to give tetragonal distortions. The four shaded surrounding atoms were allowed to relax inward (-d) and outward (+d) in the $\langle 111 \rangle$ directions.

From the calculated structure and energy parameters in Table II, it is seen that only the atoms with three extra electrons, F and Cl, favor the tetragonal structure, over trigonal. Atoms with two extra electrons, O and S, favor the trigonal structure. Of the atoms with one extra electron, N favors the trigonal structure and P shows no preference.

Focusing on the trigonal structure of N, O, and F, we see for the first two a large elongation of one bond to 2.0 and 2.1 Å and large compressions of the other three bonds to 1.41 and 1.48 Å (the diamond value is 1.54 Å). The elongations are the consequence of the nearest-neighbor antibonding nature of orbitals in the conduction band. A bond stretches to stabilize one of the N-C or O-C σ^* orbitals, but this occurs at the expense of compressing three N-C or O-C bonds. The occupied σ^* orbital is shown in Fig. 3 based on the O calculation. When a third extra electron is brought in with F, the trigonal structure is maintained, and the other three bonds stretch as shown in Table II. However, more stability is achieved in the tetragonal structure with two very long bonds of 2.1 Å and two short ones at 1.4 Å. This allows two σ^* orbitals to drop deep into the band gap, one for a doubly

TABLE V. Calculated bonding energies for atoms A and B in the relaxed divacancy site, $BE(V_2)$ (eV), and in monovacancy sites $BE(2V)$ (eV), $AB(s)$ dissociation energies ΔE (eV) as defined in Eqs. (6) and (7), and structure parameters as defined in Fig. 4 for the optimized defect structures. All displacements from lattice points d_i and internuclear and other distances R are in Å and angles in degrees. Carbon atoms that are next-nearest neighbors to substitutional atoms A and B are constrained to the bulk diamond lattice sites.

Dimer	$BE(V_2)$	$BE(2V)$	ΔE	R_{A-B}	α	R_α	β	R_β	d_1	$d_{2,3}$	d_4	$d_{3,6}$	R_{A-1}	$R_{A-2,3}$	R_{B-4}	$R_{B-5,6}$
BO	17.92	18.28	3.09	1.482	9.88	1.507	0.98	1.519	0.025	0.005	0.251	0.006	1.552	1.539	2.052	1.458
BS	8.06	5.56	5.95	1.652	0.50	1.674	0.50	1.518	0.057	0.037	0.175	0.161	1.571	1.530	1.735	1.703
NO	15.99	17.23	1.69	2.099	10.00	1.844	0.00	1.798	-0.002	-0.004	0.239	0.019	1.472	1.470	2.023	1.362
NS	5.65	5.03	4.07	1.453	0.03	1.508	-12.31	1.484	0.104	0.291	0.144	0.164	1.374	2.025	1.704	1.724
BeCl	6.98	-0.27	10.70	1.560	5.85	1.622	0.43	1.477	0.091	0.048	0.348	0.139	1.617	1.558	2.053	1.639

TABLE VI. Calculated structure parameters for $AB^+(s)$. See Fig. 4 and caption to Table V.

Dimer	R_{AB}	α	R_a	β	R_B	d_1	$d_{2,3}$	d_4	$d_{5,6}$	$R_{A=1}$	$R_{A=2,3}$	$R_{B=4}$	$R_{B=5,6}$
BO^+	1.662	0.00	1.540	0.00	1.602	-0.001	-0.001	0.000	0.000	1.539	1.539	1.521	1.521
BS^+	1.605	0.50	1.678	0.50	1.526	0.040	0.044	0.156	0.165	1.554	1.536	1.713	1.704
NO^+	2.114	0.00	1.862	0.00	1.791	-0.004	-0.004	-0.015	-0.016	1.472	1.472	1.450	1.450
NS^+	1.507	0.03	1.594	12.30	1.451	0.275	0.049	0.156	0.136	2.134	1.454	1.729	1.708
$BeCl^+$	1.608	0.00	1.525	0.00	1.623	0.045	0.045	0.113	0.113	1.559	1.559	1.658	1.658

occupied and the other for a singly occupied orbital. These orbitals are shown in Fig. 3 based on the Cl calculation: For Cl the a_1 orbital is singly occupied, and the b_2 orbital is doubly occupied; for F the order is reversed.

Moving now to P, S, and Cl, the near equality of stabilities for the trigonal and tetragonal structures of substitutional P reflects the large size of the P atom. The lengthening of the P-C bond for the trigonal structure is small compared to our finding for substitutional N, and the other three bonds are shortened only slightly. Being smaller, S does not have such a strong isotropic component to its force against the lattice (prior to relaxation) and for the trigonal structure one bond is able to stretch considerably to 2.2 Å, accommodating the two band-gap electrons in a S-C σ^* orbital, while the other three S-C bonds compress to 1.45 Å. Substitutional Cl favors the tetragonal structures with two bonds quite long at 2.1 Å, and the other two at 1.6 Å. As Fig. 4 shows, the sequence of donor levels lies higher for P, S, and Cl than for N, O, and F, and this is dominated by the larger orbital sizes of the former, though reduced atomic ionization potentials, which affect the ASEED-MO parameterization, also contribute.

The optical excitation energies, based on the energy levels shown in Fig. 4, are listed in Table III along with the relaxation energies based on optimizing the AC_{70}^+ clusters and the C_{98}^- cluster and the thermal excitation energies, which are calculated as the sum of the optical and relaxation energies. Of the set, only P is predicted to be a shallow optical donor, and both P and Cl are shallow thermal donors.

The calculated relaxation energies are relatively large for N, S, and Cl, and in fact for Cl the relaxation energy causes a change from deep optical to shallow thermal donor. The relaxation energies are the result of ionization from an orbital that is very antibonding and has caused large distortion away from the diamond lattice structure. Relaxed structures of the AC_{70}^+ clusters in Table IV compared with the initial state structures in Table II show how large stability gains occur for those cases where there are large structure changes. For N, removal of the band-gap electron allows the 2.00-Å N-C bond and the three compressed 1.41-Å bonds to all relax to 1.52 Å, with N⁺ sitting in the tetrahedral site. This relaxation gives 2.63 eV of greater stability. Because P is larger than N, relaxations with substitutional P are smaller. For O, relaxations of structure and energy are small because after ionization one electron still remains in a O-C σ^* orbital, so the stretched O-C bond remains long. For S the two band-gap electrons settle in a very stretched (2.20 Å) S-C σ^* bonding orbital, and upon ionization the structure relaxes to one similar to P with relatively small S-C bondlength variations. When an electron is removed from F, which has two 2.09-Å bonds in the tetragonal structure, a trigonal structure with a long F-C bond forms. Substitutional Cl experiences similar

structure change when ionized, but with a large relaxation stabilization because of its large compressive energy against the surrounding lattice when two Cl-C bonds are long.

B. Substitutional heteroatom pairs in divacancy sites: BO, BS, BeCl, NO, and NS

Structure parameters for these systems, as defined in Fig. 5, are given in Table V along with stabilities relative to isolated substitutional atom states. Calculated optical excitation energies, relaxation energies, and thermal excitation energies are given in Table III. All five substitutional dimers are calculated to be stable with respect to dissociation [Eq. (6)]. That is, the energy changes, ΔE in Table V, are all positive. Binding energies of $A+B$ in divacancy sites compared to isolated monovacancy sites are higher for BS, NS, and BeCl and lower for BC and NO. The difference between these binding energies is another measure of the relative stabilities of the associated and dissociated substitutional defects. The dissociation process of Eq. (6) favors the associated pairs in part because V_2 has one more C-C bond than 2 V and in our calculations the strength of this bond is 3.45 eV. The implication of these results is that when the dimers form during growth they are likely to be robust.

The above results can be analyzed using what we learned about substitutional atom defects in Sec. V A. The substitutional BO defect is isoelectronic with the substitutional CN defect, and since B and C are adjacent in the Periodic Table and relatively close in size, as are O and N, deep donor properties are predicted just as for N, and the O-C bond is elongated just as the N-C bond is. The ionized defect BO^+ takes trigonal symmetry (Table VI) about B and O. The BS defect behaves like substitutional CP, with which it is isoelectronic and shares a similar size. Because of the large size of sulfur, a band-gap orbital, involving a stretched B-C or S-C bond does not form, and when ionized the structure is not quite trigonal. The NO defect is similar to CF in that it is calculated to be a deep optical and thermal donor. Substitutional F takes a tetragonal structure with two very long (2.09 Å) and two very short (1.39 Å) bonds to C. N is in a roughly trigonal orientation, with three N-C bonds of the same (1.47 Å) length and the NO bond long at 2.10 Å; O has one long (2.02 Å) O-C bond and two short (1.36 Å) bonds. With this pseudotetragonal distortion about O, the doubly occupied orbital has become about 1 eV more stable (Fig. 6) than the trigonal O level in Fig. 4. When ionized, the structures about N and O are trigonal. Substitutional NS, being similar to CCl, is calculated to be a shallow thermal donor, like CCl, and a deep optical donor. It has a pseudotetragonal structure with two long 2.02-Å N-C bonds. When NS is ionized, the structure becomes pseudotrigonal with one long N-C bond

due to the large size of S. The ionized NO defect, on the other hand, has a readily recognizable trigonal structure. Finally, BeCl, which is similar to CP, is, unlike it, a deep optical donor but, since the long (2.05 Å) C-Cl bond can relax 0.50 Å on ionization, there is a large (2.30 eV) relaxation energy that renders BeCl a potential shallow thermal donor. The ionized defect takes on trigonal symmetry.

C. Large atoms in divacancy sites: I and Xe

As explained in Sec. I, I should promote one, and Xe two electrons into band-gap orbitals when in divacancy sites. This is seen in Fig. 6, and from Table III we see that both are expected to be deep optical donors, and I, but not Xe, is predicted to be a shallow thermal donor. With respect to the free atom states, I binds with a stability of 1.42 eV, and Xe is unstable by 4.49 eV. I fits well in this site, with the inversion center of the V_2 site retained. The relaxation of the two C atoms at each end is increased by 0.06 Å to 0.154 Å and for the third C atom the relaxation is decreased by 0.103 Å to 0.068 Å. Nearest neighbor I-C bond lengths are four at 2.085 Å and two at 2.001 Å. These are close to the methyl iodide value of 2.13 Å. Around I⁺ all C-I bonds are 2.013 Å long and all C relaxations away are 0.068 Å. Xe has moved well off center, so that it is 1.774 Å from three neighboring C and 2.515 Å from the other three. Being close to three carbon atoms satisfies its smaller atomic radius. It forms bonds with these C atoms and three electrons are sent to the three dangling half-filled orbitals centered 2.315 Å away, so that they become fully occupied. These orbitals are shown in Fig. 7 along with iodine's donor orbital for comparison.

VI. CONCLUDING COMMENTS

Our study provides a motivation for attempting to create shallow donors in diamond by incorporation of I and Cl, and the pairs B with S, N with S, and Be with Cl. It may be possible to form them by kinetic trapping during low-pressure growth or by ion implantation.

Generally, we find that large substitutional atom size is a prerequisite for shallow thermal doping. Half-filled donor levels are more likely to be shallow donors because they are destabilized more, being antibonding counterparts in situations where there is a bond order of $\frac{1}{2}$. Double occupation means zero bond order, and the atoms can move further apart, stabilizing the donor orbital until the restoring force of

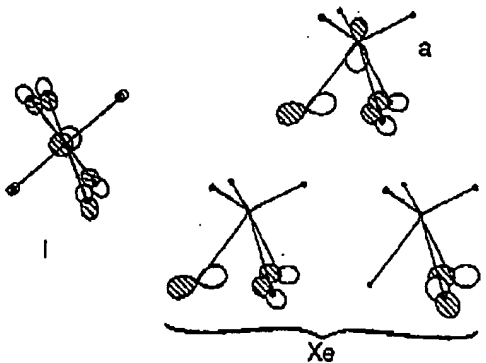


FIG. 7. Donor orbital for I in the center of the divacancy site and a - and e -symmetry band-gap orbitals for Xe in the off-center position within the divacancy site.

the lattice prevents further separation. Thus P, with one band-gap electron, is predicted to be a shallow donor, and S, with two, is a deep donor, whereas the small atoms N and O are both deep donors. The three-band-gap-electron atom Cl is calculated to be a shallow donor because of a large relaxation from tetragonal to trigonal structure upon ionization. F, on the other hand, is a deep donor because of its small size and relatively stable occupied band gap orbitals.

For the substitutional dimers, results are similar to those obtained for the monomers. Each of these dimers has at least one first row atom. Thus BO is like N, has one band-gap electron and is a deep donor, while isoelectronic BS is like P and is a shallow donor, as is also the case for BeCl. The three-band-gap-electron dimer NO is like F and is a deep donor, whereas NS is like Cl, a shallow donor.

Finally, I in the divacancy site has a single electron high in the band gap and is a shallow donor. Its large size is responsible. The donor orbital containing two electrons for Xe is low in the gap because of this atom's small size and it is a deep donor.

ACKNOWLEDGMENTS

This work was supported by the National Science Foundation, Grant No. DMR-03527, and by the Chemistry Department of Case Western Reserve University. Discussions with Lubomir Kostadinov are acknowledged.

- ¹*On leave from Institute of Physical Chemistry, Bulgarian Academy of Sciences, Sofia, Bulgaria 1113.
- ¹S. P. Mehandru and A. B. Anderson, *J. Mater. Res.* **9**, 383 (1994). This paper illustrates the bonding principle and reviews the literature concerning substitutional N atoms.
- ²G. Popovici and M. A. Prelas, *Diamond Relat. Mater.* **4**, 1303 (1995). This is a brief review of research toward synthesizing *n*-type diamond from a phenomenological point of view.
- ³A. T. Collins and E. C. Lightowlers, in *The Properties of Diamond*, edited by J. E. Field (Academic, London, 1979).
- ⁴S. A. Kajihara, A. Antonelli, J. Bamhole, and R. Car, *Phys. Rev. Lett.* **66**, 2010 (1991).
- ⁵A. B. Anderson and S. P. Mehandru, *Phys. Rev. B* **48**, 4423 (1993).
- ⁶K. Okumura, J. Mort, and M. Machonkin, *Appl. Phys. Lett.* **57**, 1907 (1990).
- ⁷K. Okano, H. Kiyota, T. Iwasaki, Y. Nakamura, Y. Akiba, T. Karosa, M. Iida, and T. Nakamura, *Appl. Phys. A* **51**, 344 (1990).
- ⁸S. N. Schauer, J. R. Flemish, R. Wittstruck, M. L. Landstrass, and M. A. Piano, *Appl. Phys. Lett.* **64**, 1094 (1994).
- ⁹J. F. Prins, *Diamond Relat. Mater.* **4**, 580 (1995).
- ¹⁰G. Z. Cao, F. A. J. M. Dricesen, G. J. Bonthuis, L. J. Giling, and P. F. A. Alkemade, *J. Appl. Phys.* **73**, 3125 (1995).
- ¹¹A. B. Anderson and L. Kostadinov, *J. Appl. Phys.* (to be published).
- ¹²S. M. Gorbaikin, R. A. Zehr, J. Roth, and H. Naramoto, *J. Appl. Phys.* **70**, 2986 (1991).

14 348

ANDERSON, GRANTSCHAROVA, AND ANGUS

54

¹³K. Bharuth-Ram, H. Quintel, M. Restle, C. Ronning, H. Hoffässer, and S. G. Jahn, *J. Appl. Phys.* **78**, 5180 (1995).

¹⁴J. D. Hunn, N. R. Parkh, M. L. Swanson, and R. A. Zur, *Diamond Relat. Mater.* **2**, 847 (1993).

¹⁵S. P. Mehandru, A. B. Anderson, and J. C. Angus, *J. Mater. Res.* **7**, 689 (1992).

¹⁶M. Restle, K. Bharuth-Ram, H. Quintel, C. Ronning, S. G. Jahn, and U. Wahl, *Appl. Phys. Lett.* **66**, 2733 (1995).

¹⁷A. B. Anderson, *J. Chem. Phys.* **62**, 1187 (1975); A. B. Anderson, R. W. Grimes, and S. Y. Hong, *J. Phys. Chem.* **91**, 4245 (1987); A. B. Anderson, *Int. J. Quantum Chem.* **49**, 581 (1994).

¹⁸K. Nath and A. B. Anderson, *Solid State Commun.* **66**, 277 (1988).

¹⁹K. J. Chang and M. L. Cohen, *Phys. Rev. B* **35**, 8196 (1987); M. T. Yin and M. L. Cohen, *ibid.* **26**, 5668 (1982).